Monthly Notices of the ROYAL ASTRONOMICAL SOCIETY
MNRAS **445,** 2994–2998 (2014) doi:10.1093/mnras/stu2144

NGC 6522: a typical globular cluster in the Galactic bulge without signatures of rapidly rotating Population III stars

Melissa Ness,[1⋆] Martin Asplund[2] and Andrew R. Casey[3]

[1]*Max-Planck-Institut für Astronomie, Königstuhl 17, D-69117 Heidelberg, Germany*
[2]*Research School of Astronomy and Astrophysics, Australian National University, Cotter Road, Weston Creek, ACT 2611, Australia*
[3]*Institute of Astronomy, University of Cambridge, Madingley Road, Cambridge CB3 0HA, UK*

Accepted 2014 September 5. Received 2014 September 5; in original form 2014 August 1

ABSTRACT

We present an abundance analysis of eight potential member stars of the old Galactic bulge globular cluster NGC 6522. The same stars have previously been studied by Chiappini et al., who found very high abundances of the slow neutron capture elements compared with other clusters and field stars of similar metallicity, which they interpreted as reflecting nucleosynthesis in rapidly rotating, massive Population III stars. In contrast to their analysis, we do not find any unusual enhancements of the neutron capture elements Sr, Y, Ba and Eu and conclude that previous claims result mainly from not properly accounting for blending lines. Instead, we find NGC 6522 to be an unremarkable globular cluster with comparable abundance trends to other Galactic globular clusters at the same metallicity ([Fe/H] $= -1.15 \pm 0.16$). The stars are also chemically similar to halo and bulge field stars at the same metallicity, spanning a small range in [Y/Ba] and with normal α-element abundances. We thus find no observational evidence for any chemical signatures of rapidly rotating Population III stars in NGC 6522.

Key words: stars: abundances – stars: Population III – Galaxy: abundances – Galaxy: bulge – globular clusters: general.

1 INTRODUCTION

As one of the oldest stellar populations in our Galaxy, globular clusters are key to understanding the earliest epochs of galaxy evolution and stellar nucleosynthesis. Globular clusters may therefore contain unique chemical markers of the first generations of stars. All globular clusters indeed show abundance peculiarities compared with the typical field population, such as an O–Na anticorrelation, which is normally interpreted as reflecting two or more generations of stars in the clusters with the first one sharing the chemical composition with normal field stars of the same metallicity (Gratton, Carretta & Bragaglia 2012).

The nature of the polluter of the later generations of stars is still being debated with intermediate mass asymptotic giant branch stars or rapidly rotating massive stars the leading contenders. As the polluters would be part of the first cluster generation, some of which are still present, they would thus not be metal-free Population III stars but Population II stars of the same metallicity as the cluster as a whole. Until recently, there have been no convincing observations of Population III nucleosynthesis in any globular cluster star but Chiappini et al. (2011) claim to have found exactly such a smoking gun in NGC 6522.

NGC 6522 is a little studied globular cluster in the Milky Way's bulge. Observations of individual stars in this cluster are difficult due to the large crowding of more metal-rich bulge stars and foreground disc contamination in this region as well as the heavy interstellar extinction and reddening characteristic of sight lines of the Galactic bulge, especially near the plane. However, this is a particularly important globular cluster because it may be the oldest globular cluster in the Milky Way (Barbuy et al. 2009), and it may contain vital clues to the formation and early evolution of the still poorly understood bulge (e.g. Ness et al. 2013). Chiappini et al. (2011) recently analysed eight potential NGC 6522 cluster members and found remarkably high abundances of slow neutron-capture elements, distinct from any other globular cluster observed. The authors demonstrated that such a chemical abundance pattern would be consistent with the nucleosynthesis predicted for rapidly rotating massive, extremely metal-poor or Population III stars, so-called spinstars (Pignatari et al. 2008).

The fact that this cluster is so far unique in carrying such a nucleosynthetic signature may reflect that the very first stars born after the big bang formed in the largest overdensities, which subsequently grew with time to become centres of galaxies. The oldest Galactic stars should therefore be concentrated in the bulge region (Tumlinson 2010), which also experienced the most rapid chemical enrichment due to the intense star formation rate, making it conceivable that any Population III chemical fingerprint may preferentially show up in an old bulge cluster with [Fe/H] ≈ -1 such as NGC 6522.

Given the potentially far-reaching implications of the work of Chiappini et al. (2011), we present a re-analysis of the same cluster stars but importantly with a more detailed accounting of blending

⋆E-mail: ness@mpia.de

lines as well as isotopic hyperfine splitting (HFS) of the *s*-process abundance diagnostics.

2 OBSERVATIONS

The GIRAFFE/VLT data from the programme 071.B-0617(A) (PI = A. Renzini) were downloaded from the ESO archive. These observations were taken during 2003 May–July and comprised of two-field pointings and three wavelength settings: HR13 (612–640 nm), HR14 (638.3–662.6 nm) and HR15 (679.7–696.5 nm). A more comprehensive description of the data can be found in Barbuy et al. (2009). A number of calibration frames were missing from the ESO archive but were provided by ESO support upon request. We could not locate all of the data corresponding to the total exposure times reported in Barbuy et al. (2009) for unknown reasons. The available data were reduced using GASGANO (version 1.24) with the wavelength calibration verified using skylines and telluric lines. The data were sky subtracted using an automated python routine that determined a median sky from the available sky fibres and removed it from each science frame. For each wavelength setting, separate frames were co-added. The resulting signal-to-noise ratio (S/N) per resolution element for the three wavelength settings are listed in Table 1.

The stellar radial velocities were determined from a cross-correlation with a theoretical model atmosphere spectrum (corresponding to $T_{\rm eff}$ = 5000 K, $\log g$ = 3.0 [cgs], [Fe/H]=−1.0) smoothed to the resolving power of the observations using the routine FXCOR in PYRAF. Bad pixels and telluric regions were masked out for this procedure. Our measured radial and heliocentric velocities are listed in Table 1. The mean heliocentric velocity we report for these nine candidate NGC 6522 stars is $\langle V_{\rm helio}\rangle = -13.4 \pm 4.9$ km s^{-1}, which is in reasonable agreement with the value quoted by Harris (1996): -21.1 ± 3.4 km s^{-1}. It is possible that some of the candidate stars may not be cluster members in spite of the similarity in velocity and metallicity, although there is some discussion in the literature regarding the actual heliocentric velocity of the cluster (Terndrup et al. 1998). It should be noted that our heliocentric velocities differ from those reported by Barbuy et al. (2009) based on the same observations. Our inferred heliocentric velocities from the three different wavelength settings obtained at different times are in excellent agreement with each other ($\sigma < 0.7$ km s^{-1}), which is not true for Barbuy et al. (2009, see their table 3). This difference comes from an error in the original analysis of Barbuy et al. (2009), discussed in Barbuy et al. (2014).

Table 1. Summary of the measured velocities the nine NGC 6522 candidate members.

Star	Grating (J2000)	S/N	$V_{\rm rad}$ (km s^{-1})	$V_{\rm helio}$ (km s^{-1})	$\langle V_{\rm helio}\rangle$ (km s^{-1})	$\sigma(V_{\rm helio})$ (km s^{-1})
B-008	HR13	88	−29.9	−8.8	−8.6	0.3
	HR14	81	−8.6	−8.6		
	HR15	132	−16.0	−8.2		
B-107	HR13	93	−27.0	−5.9	−6.0	0.4
	HR14	86	−6.5	−6.5		
	HR15	134	−13.3	−5.5		
B-108	HR13	156	−33.1	−12.1	−13.0	0.7
	HR14	142	−13.7	−13.8		
	HR15	188	−20.9	−13.1		
B-118	HR13	87	−42.9	−21.9	−21.9	0.1
	HR14	85	−22.0	−22.0		
	HR15	133	−29.7	−21.9		
B-122	HR13	96	−36.9	−15.8	−15.7	0.1
	HR14	92	−15.6	−15.7		
	HR15	134	−23.3	−15.5		
B-128	HR13	84	−33.9	−12.9	−12.6	0.3
	HR14	83	−12.7	−12.7		
	HR15	119	−19.9	−12.1		
B-130	HR13	77	−36.6	−15.6	−15.6	0.2
	HR14	71	−15.3	−15.4		
	HR15	117	− 23.7	−15.9		
B-134	HR13	84	−39.4	−18.4	−18.9	0.4
	HR14	81	−19.3	−19.4		
	HR15	127	−26.8	−18.9		
F-121	HR13	58	−14.1	−8.7	−8.8	0.2
	HR14	93	4.3	−8.6		
	HR15	140	−7.3	−9.1		

3 ABUNDANCE ANALYSIS

After continuum normalization, we performed a standard 1D local thermodynamic equilibrium abundance analysis using the SMH spectrum analysis program of Casey (2014), which is built around the well-known MOOG code of Sneden (1973). Initial effective temperature guesses were provided by de-reddened 2MASS photometry (Skrutskie et al. 2006) using the Bessell, Castelli & Plez (1998) calibration. Similarly to Barbuy et al. (2009), we discard the star B-134 from further analysis due to contamination of the spectra from a companion/blending star. Spectroscopic stellar parameters of $T_{\rm eff}$, $\log g$ and [Fe/H] were determined from an iterative procedure to achieve excitation and ionization balance using ∼60 Fe I lines and 7 Fe II lines. The microturbulence parameter ($\xi_{\rm turb}$) was calculated by removing any abundance trends with reduced equivalent width. The final stellar parameters are reported in Table 2. The typical uncertainties in the stellar parameters are $\sigma(T_{\rm eff}) = 80$ K, $\sigma(\log g) = 0.20$ and $\sigma([{\rm Fe/H}]) = 0.15$, respectively. We report a marginally lower mean metallicity for these eight stars than Barbuy et al. (2009): $[{\rm Fe/H}] = -1.15 \pm 0.16$ compared to $[{\rm Fe/H}] = -1.00 \pm 0.20$.

Individual abundances were determined from the equivalent widths of unblended lines for which reliable oscillator strengths were available from the *Gaia*-ESO line list (Heiter et al., in preparation). In the limited wavelength regions of these GIRAFFE observations, we made use of 22 lines of the α-elements (Mg, Si, Ca, Ti), two lines available for Al, two for Na, two for Ba, three for Eu, one for La and one for Y. For the neutron capture elements, we performed spectrum synthesis taking care of including isotopic and HFS and blending lines to ensure the most reliable results. Our mean elemental abundance measurements are given in Table 3 while the full line-by-line results are provided in Table 4 (online only). We estimate the uncertainties on individual abundances from the

Table 2. Summary of derived stellar parameters.

Star	$T_{\rm eff}$	$\log g$	[Fe/H]	$\xi_{\rm turb}$
B-008	4960	2.65	−1.02	2.3
B-107	4970	1.9	−1.34	2.1
B-108	4750	2.2	−1.37	1.4
B-118	5000	2.25	−1.04	2.45
B-122	5100	2.75	−0.95	1.2
B-128	4760	2.1	−1.02	1.3
B-130	5090	2.65	−1.23	2.8
F-121	4955	2.2	−1.0	1.4

Table 3. Summary of measured abundances for individual elements for the eight candidate NGC 6522 stars. The measurement for each star is in the first row and the upper and lower errors of the measurement are in the two following rows.

Star	[Fe/H]	[Fe I/H]	[Fe II/H]	[Na I/Fe]	[Mg I/Fe]	[Al I/Fe]	[Si I/Fe]	[Ca I/Fe]	[Ti I/Fe]	[Y II/Fe]	[Ba II/Fe]	[La II/Fe]	[Eu II/Fe]
B-008	− 1.02	− 1.02	− 1.03	0.68	0.23	1.0	0.30	0.25	0.46	0.35	0.45	0.70	0.70
	+0.15	+0.15	+0.15	+0.1	+0.2	+0.1	+ 0.1	+0.2	+0.1	+0.2	+0.1	+0.15	+0.15
	− 0.15	− 0.15	− 0.15	− 0.1	− 0.2	− 0.1	− 0.1	− 0.2	− 0.1	− 0.3	− 0.1	− 0.2	− 0.15
B-107	− 1.34	− 1.34	− 1.34	0.13	0.51	0.49	0.52	0.34	0.27	0.15	0.40	0.30	0.25
	+0.15	+0.15	+0.15	+0.25	+0.2	+0.25	+0.15	+0.15	+0.1	+0.25	+0.1	+0.2	+0.15
	− 0.15	− 0.15	− 0.15	− 0.30	− 0.25	− 0.25	− 0.15	− 0.15	− 0.1	− 0.30	− 0.1	− 0.25	− 0.15
B-108	− 1.37	− 1.37	− 1.37	− 0.23	0.63	0.26	0.18	0.38	0.37	0.15	0.10	0.35	0.40
	+0.15	+0.15	+0.15	+0.15	+0.15	+0.15	+0.15	+0.15	+0.15	− 0.05	+0.15	+0.25	+0.15
	− 0.15	− 0.15	− 0.15	− 0.15	− 0.15	− 0.40	− 0.40	− 0.15	− 0.15	− 0.05	− 0.15	− 0.45	− 0.2
B-118	− 1.04	− 1.04	− 1.04	0.40	0.37	1.01	0.29	0.28	0.54	0.30	0.30	0.55	0.40
	+0.15	+0.15	+0.15	+0.1	+0.1	+0.1	+0.1	+0.15	+0.15	+0.2	+0.1	+0.1	+0.15
	− 0.15	− 0.15	− 0.15	− 0.1	− 0.1	− 0.1	− 0.1	− 0.15	− 0.15	− 0.30	− 0.1	− 0.1	− 0.15
B-122	− 0.95	− 0.95	− 0.95	0.42	0.36	0.62	0.21	0.29	0.33	0.10	0.35	0.30	0.50
	+0.15	+0.15	+0.15	+0.1	+0.15	+0.1	+0.15	+0.15	+0.1	+0.25	+0.1	+0.1	+0.15
	− 0.15	− 0.15	− 0.15	− 0.1	− 0.15	− 0.1	− 0.15	− 0.15	− 0.1	− 0.35	− 0.1	− 0.15	− 0.15
B-128	− 1.02	− 1.03	− 1.03	0.20	0.34	0.82	0.21	0.50	0.25	0.40	0.80	0.30	0.0
	+0.1	+0.1	+0.1	+0.15	+0.15	+0.1	+0.15	+0.15	+0.1	+0.2	+0.1	+0.15	+0.15
	− 0.1	− 0.1	− 0.1	− 0.15	− 0.15	− 0.1	− 0.15	− 0.15	− 0.1	− 0.25	− 0.1	− 0.15	− 0.15
B-130	− 1.23	− 1.24	− 1.24	0.46	0.34	0.64	0.32	0.35	0.40	0.44	0.10	0.45	0.90
	+0.15	+0.15	+0.15	+0.15	+0.25	+0.2	+0.2	+0.15	+0.1	+0.25	+0.1	+0.2	+0.15
	− 0.15	− 0.15	− 0.15	− 0.25	− 0.25	− 0.2	− 0.2	− 0.15	− 0.1	− 0.30	− 0.1	− 0.2	− 0.15
F-121	− 1.0	− 0.99	− 1.01	− 0.11	0.54	0.12	0.20	0.43	0.42	0.20	0.45	0.10	0.30
	+0.15	+0.15	+0.15	+0.20	+0.2	+0.2	+0.15	+0.15	+0.15	+0.2	+0.2	+0.1	+0.10
	− 0.15	− 0.15	− 0.15	− 0.3	− 0.15	− 0.2	− 0.15	− 0.15	− 0.15	− 0.25	− 0.2	− 0.1	− 0.15

Table 4. Excerpt of table of individual line measurements for each star. The full table is available as Supplementary Material online.

Rest wavelength (Å)	Transition	Element	Excitation potential (eV)	Oscillator strength	Equivalent width (mÅ)	Abundance (dex)
Star B-008						
6122.217	20.0	Ca I	1.89	−0.316	176.62	5.44
6126.216	22.0	Ti I	1.07	−1.368	49.73	4.36
6127.906	26.0	Fe I	4.14	−1.399	37.15	6.50
6137.691	26.0	Fe I	2.59	−1.402	145.72	6.33
6149.246	26.1	Fe II	3.89	−2.841	19.99	6.52

quadrature sum of the uncertainties due to the noise in the spectra, and the uncertainties in the stellar parameters and the line-to-line dispersion. These are listed in Table 3.

In general, we find comparable stellar abundances to Barbuy et al. (2009), with marginally lower [Fe/H] (by 0.15 dex) and slightly higher [α/Fe] ratios (by ≈0.2 dex). Our mean measurement of the α-elements of [Si/Fe], [Ti/Fe], [Ca/Fe] and [Mg/Fe] is ≈0.35 dex, compared to the mean α-abundance from these elements of ≈0.2 dex from Barbuy et al. (2009). The differences in abundance results can likely be traced to the adopted line-lists and difference in adopted stellar parameters (our $T_{\rm eff}$ and $\xi_{\rm turb}$ are typically 200 K and 0.6 km s^{-1}, respectively, higher). Similarly, our mean [Na/Fe] abundance measurement of 0.25 dex is higher than that of Barbuy et al. (2009) by about 0.2 dex, although our mean [La/Fe] and [Eu/Fe] values are comparable, measuring in both cases about 0.4 dex on average. We find a lower Ba abundance compared to Barbuy et al. (2009). The inclusion of HFS makes only a small difference to the measurements. Our mean measurement for Ba is [Ba/Fe] = 0.35 ± 0.2, compared to [Ba/Fe] = 0.5 ± 0.4 in the original analysis.

A more striking discrepancy is obtained for Y compared to the analysis of Chiappini et al. (2011). Our mean ratio is [Y/Fe] = 0.25 ± 0.10 compared to [Y/Fe] = 1.2 ± 0.2 in their analysis. Here, the difference is largely due to adopted Y lines. In our analysis, we use a single unblended Y II line at 679.54 nm, whereas the original analysis relied on the Y II line at 661.37 nm, which they did not realize is severely blended by in particular an Fe line at 661.38 nm and a Ti line at 661.36 nm (see Fig. 1). We obtain a higher abundance of [Y/Fe] by about +0.6 dex when fitting for [Y/Fe] at 661.37 nm without accounting for the blending lines.

Finally, we argue that no reliable Sr abundance can be inferred from these individual GIRAFFE spectra. Chiappini et al. (2011) relied on the Sr I 650.40 nm line, which in our opinion is not discernible over the noise of the individual spectra and is blended. This feature, for the median combination of all eight stars is shown in Fig. 2, synthesized with 0–0.6 dex of [Sr/Fe] enhancement and a fixed [V/Fe] = 0. A good fit is obtained with an [Sr/Fe] = 0.4 given a [V/Fe] = 0. The four Sr lines in the *Gaia*-ESO line-list available in this wavelength region (640.85, 655.02, 654.68, 661.73, 671.91 nm) are also too weak for abundance purposes. As a result, we do not quote any [Sr/Fe] values.

We also find discrepancies between our measured abundances and those in the reanalysis of four of the cluster members in Barbuy et al. (2014), although there is much better agreement in abundances of [Y/Fe] and [Ba/Fe]. Our [Y/Fe] measurements agree with those

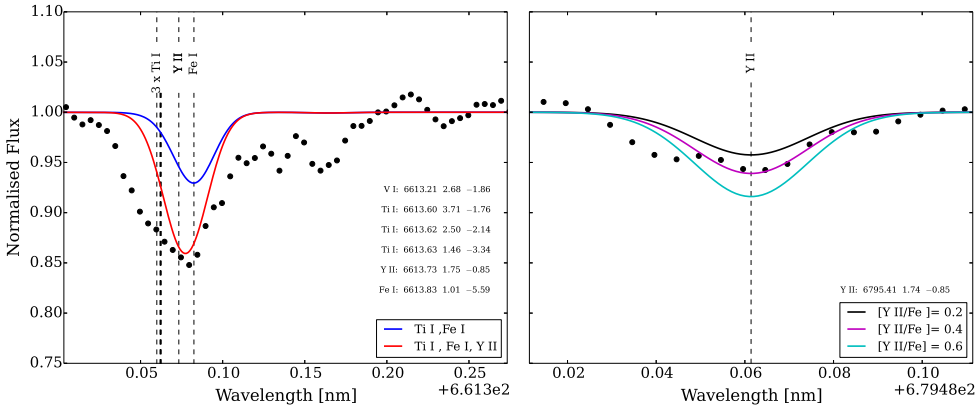

Figure 1. The blended Y II feature, which is very similar for all stars, is shown for star B-128. The panel at left shows the synthesis of this line with the contribution of Ti I and Fe I in blue and the contribution of Ti I, Fe I and Y II in red, for the Y value measured for this star shown at right, of [Y/Fe] = 0.4 dex (and [Ti/Fe] = 0.25 as measured from the Ti lines in the spectra). The panel at right shows the best-fitting abundance of [Y/Fe] = 0.4 dex and syntheses at ±0.2 dex comparison, for the unblended feature at 679.4 nm which we use to derive all of our [Y/Fe] abundances. The parameters of the absorption features are provided in the figures, to indicate the relative line strengths, in order of element, wavelength, excitation potential and log *gf*.

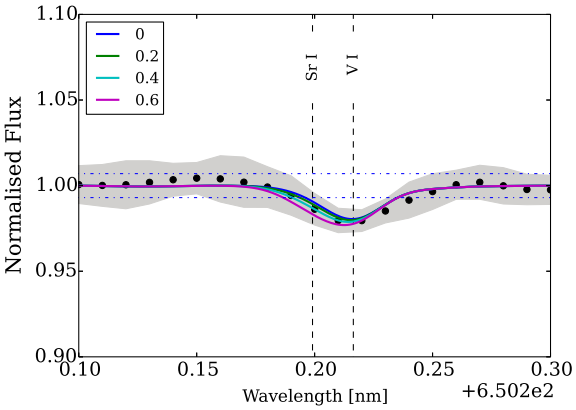

Figure 2. The median spectra from all eight stars combined for the Sr feature at 650.4 nm. The synthesis shows the line profiles for abundance ratios of [Sr/Fe] = 0,0.2,0.4,0.6 for the typical [V/Fe] ratio of [V/Fe] ≈0 for the stars. The solid grey lines represent the 1σ measurement of the mean of the eight stars and the dashed lines either side of the line profile show the width of the noise of the combined spectra. The best fit to the line adopting [V/Fe] = 0 is [Sr/Fe] = 0.40.

of Barbuy et al. (2014) for the four stars within the errors, with a mean value of ≈0.3 dex for both analyses. The difference in our individual [Ba/Fe] measurements compared to those of Barbuy et al. (2014) marginally exceed the measurement errors for the four stars, but the mean [Ba/Fe] value is similar, at ≈0.32 dex in Barbuy et al. (2014) and ≈0.4 dex for the four stars in our analysis. The measurement of [La/Fe] is also within measurement errors for the two analyses for three of the four stars, and we find a mean [La/Fe] of ≈0.35 dex compared to ≈0.23 dex in Barbuy et al. (2014) for these four stars. The difference in the α-abundance is larger and our [Mg/Fe] abundances are ≈0.4 dex compared to 0.23 dex on average for these stars, [Si/Fe] is ≈0.30 dex compared to ≈0.13 in their reanalysis and [Ti (I)/Fe] is ≈0.3 dex for our analysis compared to ≈0.04 dex in Barbuy et al. (2014). Barbuy et al. (2014) report a mean [Sr/Fe] measurement of ≈0.23 dex in their reanalysis, much nearer to the upper limit we place on this abundance from the GIRAFFE data, of 0.4 dex, compared to their original result of [Sr/Fe] ≈ 1.0. The largest discrepancies are found for [Al/Fe] and [Na/Fe]. We find mean abundances of ≈0.65 dex and ≈0.3 dex for [Al/Fe] and [Na/Fe], respectively, whereas Barbuy et al. (2014) find much lower mean abundances of ≈−0.11 and ≈−0.07 dex, respectively. Different wavelength regions and therefore features have been used for these abundance measurements between our analysis and Barbuy et al. (2014).

Fig. 3 compares our inferred abundance ratios for NGC 6522 to microlensed dwarf stars of the bulge from Bensby et al. (2013) as well as dwarf halo stars from Nissen & Schuster (2011), demonstrating in general a good agreement. The cluster stars show comparable abundances to the bulge for Mg, Si, Ca, Ti, Y and Ba, while the scatter is Na and Al is directly attributable to the Na–Al correlation typical for globular clusters. Our [Y/Fe] and [Ba/Fe] ratios are consistent with other globular clusters at this metallicity (e.g. Johnson, Dong & Gould 2010). Fig. 4 shows the [Y/Ba] of the eight NGC 6522 stars compared to field bulge and halo stars. The cluster stars are not anomalous compared to field stars of similar metallicity, neither in [Y/Ba] nor in their scatter, in contrast to the conclusion by Chiappini et al. (2011).

4 CONCLUSIONS

We have re-analysed available GIRAFFE/VLT spectra of eight members of the bulge globular cluster NGC 6522 from the ESO archive. We have paid particular attention to considering the effects of isotopic HFS and blending lines on the derived abundances of the *s*-process elements. We also use in some cases on more reliable, cleaner lines. As a result, our results are systematically and significantly lower than those reported by Chiappini et al. (2011), which did not consider those effects.

In all cases, the NGC 6522 stars display elemental abundances typical of field halo and bulge as well as other globular clusters of similar metallicities. We conclude that neither the normal *s*-process abundances nor the low and fairly constant [Y/Ba] ratios measured in NGC 6522 support a nucleosynthetic origin by rapidly rotating Population III stars. In terms of its chemical composition, NGC 6522 is an unremarkable globular cluster.

ACKNOWLEDGEMENTS

We appreciate helpful and stimulating discussions with Beatriz Barbuy and Cristina Chiappini. The research has received funding from the European Research Council under the European Union's

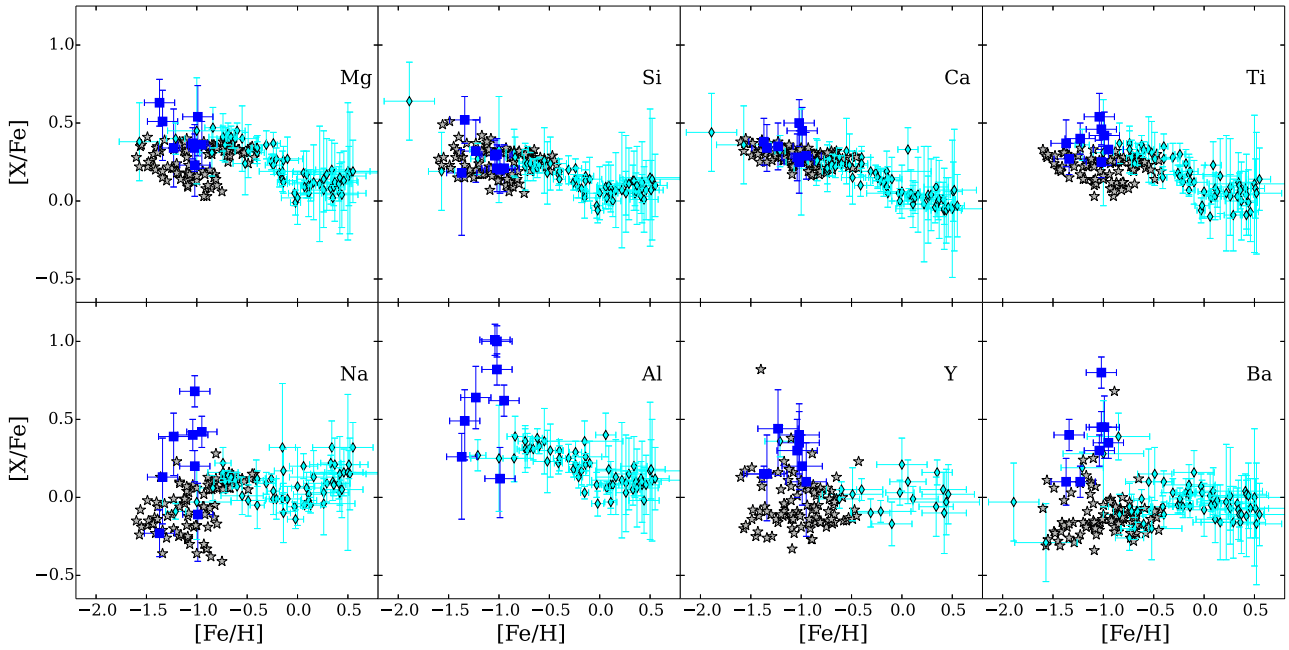

Figure 3. Comparison of Na, Mg, Ca, Si, Ti, Al, Ba and Y abundances measured for the eight stars (blue squares) compared with stars of the bulge (Bensby et al. 2013, cyan triangles) and halo stars studied by Nissen & Schuster (2011, grey stars).

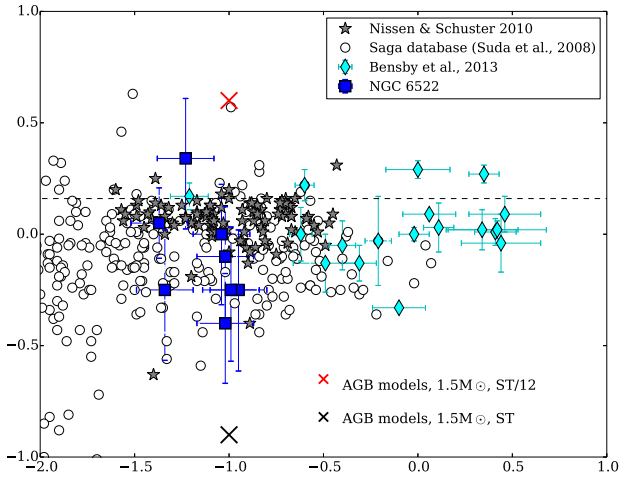

Figure 4. [Y/Ba] ratios for stars of the Galactic halo from Nissen & Schuster (2011, grey stars), the SAGA data base (Suda et al. 2008, open circles) and bulge stars of Bensby et al. (2013, cyan diamonds) compared to the eight candidate NGC 6522 stars (blue squares). Typical model predictions for the contribution of the main *r*-process is shown at 0.16 dex, along the dashed black line and the model predictions for a standard (ST) and reduced efficiency ST/12 (factor 12) AGB models are shown in the red and black crosses, respectively (see fig. 1 from Chiappini et al. (2011).

Seventh Framework Programme (FP 7) ERC Grant Agreement no. [321035]. MA acknowledges generous funding from the Australian Research Council (grant FL110100012). ARC acknowledges funding from European Research Council grant 320360: The *Gaia*-ESO Milky Way Survey.

REFERENCES

Barbuy B., Zoccali M., Ortolani S., Hill V., Minniti D., Bica E., Renzini A., Gómez A., 2009, A&A, 507, 405
Barbuy B. et al., 2014, preprint (arXiv:1408.2438)
Bensby T. et al., 2013, A&A, 549, A147
Bessell M. S., Castelli F., Plez B., 1998, A&A, 333, 231
Casey A. R., 2014, preprint (arXiv:e-prints)
Chiappini C., Frischknecht U., Meynet G., Hirschi R., Barbuy B., Pignatari M., Decressin T., Maeder A., 2011, Nature, 472, 454
Gratton R. G., Carretta E., Bragaglia A., 2012, A&AR, 20, 50
Harris W. E., 1996, AJ, 112, 1487
Johnson J. A., Dong S., Gould A., 2010, ApJ, 713, 713
Ness M. et al., 2013, MNRAS, 430, 836
Nissen P. E., Schuster W. J., 2011, VizieR Online Data Catalog, 353, 9015
Pignatari M., Gallino R., Meynet G., Hirschi R., Herwig F., Wiescher M., 2008, ApJ, 687, L95
Skrutskie M. F. et al., 2006, AJ, 131, 1163
Sneden C. A., 1973, PhD thesis, The University of Texas at Austin
Suda T. et al., 2008, PASJ, 60, 1159
Terndrup D. M., Popowski P., Gould A., Rich R. M., Sadler E. M., 1998, AJ, 115, 1476
Tumlinson J., 2010, ApJ, 708, 1398

SUPPORTING INFORMATION

Additional Supporting Information may be found in the online version of this article:

Table 4. Table of individual line measurements for each star (http://mnrasl.oxfordjournals.org/lookup/suppl/doi:10.1093/mnrasl/stu2144/-/DC1).

Please note: Oxford University Press is not responsible for the content or functionality of any supporting materials supplied by the authors. Any queries (other than missing material) should be directed to the corresponding author for the paper.

This paper has been typeset from a TEX/LATEX file prepared by the author.